fabrication. Nevertheless, the effects of the surface stress on the oxide and consequently on the lifetime and the reliability of the devices are important issues and need to be addressed further.

In the C-V traces of a MOS diode made of the Gd$_2$O$_3$ of 185 Å thickness (Fig. 4), a transition from accumulation to depletion mode occurs at $\sim$2 V. The inversion carriers (holes) follow the ac signal up to a frequency of 10 kHz and do not respond to frequencies greater than 100 kHz. This compares favorably to previous samples of Ga$_2$O$_3$(Gd$_2$O$_3$) films on GaAs, in which the inversion carriers followed the ac signal only up to a frequency of 1 kHz (*7*). There is some hysteresis in the C-V curves in reverse sweeping, with the widest spread of no more than 1 V. These curves remain the same after repeated voltage cycles.

The C-V characteristics can be further understood by taking the conductance (G) into account. The finite value of G is in parallel with the oxide capacitance (C_{ox}). This simple equivalent circuit model explains that the total capacitance increases as the modulation frequency decreases. After replotting the C-V curves by subtracting the contributions from G and C_{ox}, the D_{it}, which responds only to the low-frequency measurements, can be deduced from the high- and low-frequency curves. D_{it} at the midgap is $\sim 10^{11}$ cm^{-2} eV^{-1}, which is slightly higher than those of the SiO$_2$/Si interfaces.

We expect that epitaxial growth of structures isomorphic to that of Mn$_2$O$_3$ can be extended to other rare earth oxides and to other semiconductor substrates like Si. Our findings thus suggest new opportunities for producing high-ϵ gate dielectrics for Si- and GaAs-based MOSFETs.

References and Notes

1. A. Revesz and K. Zaininger, *J. Am. Ceram. Soc.* **46**, 606 (1963).
2. O. Weinreich, *J. Appl. Phys.* **37**, 2924 (1966).
3. T. Mimura, K. Odani, N. Yokoyama, Y. Nakayama, M. Fukuta, *IEEE Trans. Electron Devices* **25**, 573 (1978).
4. W. T. Tsang, *Appl. Phys. Lett.* **33**, 429 (1978).
5. C. W. Wilmsen, Ed., *Physics and Chemistry of III-V Compound Semiconductor Interfaces* (Plenum, New York, 1985).
6. M. Hong *et al.*, *J. Vac. Sci. Technol. B* **14**, 2297 (1996).
7. M. Passlack *et al.*, *IEEE Trans. Electron Devices* **44**, 214 (1997).
8. F. Ren *et al.*, *Technical Digest of the IEEE, International Electron Devices Meeting*, San Francisco, CA, 8 to 11 December 1996 (IEEE, Piscataway, NJ, 1996), pp. 943–945.
9. F. Ren *et al.*, *IEEE Electron Device Lett.* **19**, 309 (1998).
10. L. W. Tu, E. F. Schubert, M. Hong, G. J. Zydzik, *J. Appl. Phys.* **80**, 6448 (1996).
11. J. Kwo *et al.*, *J. Vac. Sci. Technol. B*, in press.
12. M. Hong, *J. Cryst. Growth* **150**, 277 (1995).
13. M. Hong *et al.*, *J. Vac. Sci. Technol. B* **16**, 1395 (1998).
14. A. R. Kortan, A. Erbil, R. J. Birgeneau, M. S. Dresselhaus, *Phys. Rev. Lett.* **47**, 1206 (1981).
15. S. Geller, *Acta Crystallogr. B* **27**, 821 (1971).
16. K. Nashimoto, D. K. Fork, T. H. Geballe, *Appl. Phys. Lett.* **60**, 1199 (1992).
17. Y. C. Wang, M. Hong, J. Kwo, J. P. Mannaerts, unpublished results.
18. We would like to thank A. Y. Cho, R. M. Fleming, T. S. Lay, C. T. Liu, D. W. Murphy, G. L. Timp, R. B. van Dover, Y. H. Wong, and M. C. Wu for valuable suggestions.

19 October 1998; accepted 8 February 1999

Degradation Mechanism of Small Molecule–Based Organic Light-Emitting Devices

Hany Aziz,[1] Zoran D. Popovic,[2]* Nan-Xing Hu,[2] Ah-Mee Hor,[2] Gu Xu[1]

Studies on the long-term degradation of organic light-emitting devices (OLEDs) based on tris(8-hydroxyquinoline) aluminum (AlQ$_3$), the most widely used electroluminescent molecule, reveal that injection of holes in AlQ$_3$ is the main cause of device degradation. The transport of holes into AlQ$_3$ caused a decrease in its fluorescence quantum efficiency, thus showing that cationic AlQ$_3$ species are unstable and that their degradation products are fluorescence quenchers. These findings explain the success of different approaches to stabilizing OLEDs, such as doping of the hole transport layer, introducing a buffer layer at the hole-injecting contact, and using mixed emitting layers of hole and electron transporting molecules.

Because of their high brightness (*1*, *2*) and the availability of a wide range of emission colors (*3*, *4*), OLEDs have the potential to achieve low-cost, full-color flat-panel displays. However, OLEDs show relatively poor stability. The half-lifetime, defined as the time elapsed before the luminance of the OLED decreases to half its initial value, usually amounts to only few hundred hours (*4*). In general, degradation in OLEDs occurs through the formation of nonemissive "dark" spots as well as through a long-term "intrinsic" decrease in the electroluminescence (EL) efficiency of the devices during operation (*5*). Although the mechanisms that cause dark spots have been identified (*5*, *6*) and controlled (*7*), the causes of intrinsic degradation remain unclear. In the devices based on small organic molecules, introduction of dopants in the hole transport layer (HTL) (*8*) or a buffer layer at the hole-injecting contact (*9*) was found to significantly reduce the intrinsic degradation. Half-lifetimes exceeding 4000 hours, at an initial luminance of 500 cd/m^2, have been achieved for devices with a copper phthalocyanine (CuPc) buffer layer (*9*). The life and efficiency of these devices is further extended by doping the AlQ$_3$ with *N,N*- dimethylquinacridone (*10*). Morphological changes in the HTL or degradation at the hole-injecting contact were speculated to cause degradation in the OLEDs, but the occurrence of such processes in OLEDs or their role in degradation has never been verified. In fact, other reports show no correlation between the morphological stability of the HTL and the lifetime of the OLEDs (*11*).

We investigated OLEDs based on AlQ$_3$, the most widely used electroluminescent molecule, and found that injection of holes in AlQ$_3$ was the main factor responsible for device degradation. Photoluminescence (PL) quantum efficiency of AlQ$_3$ layers, where predominantly holes are transported, decreased upon prolonged current flow (*12*). These findings naturally explain different approaches to stabilizing OLEDs, such as doping of the HTL (*8*), introducing a CuPc buffer layer at the hole-injecting contact (*9*), or using a mixed emitting layer of hole and electron transporting molecules (*13*).

We previously found that using a mixed emitting layer of hole and electron transporting molecules, placed between pure hole and electron transport layers (ETLs), dramatically increased LED stability (*13*). These devices show a half-lifetime of about 1400 hours at an initial luminance of about 1000 cd/m^2 (versus tens of hours for devices with pure layers), despite not having a doped HTL or a buffer layer at the hole-injecting contact (Fig. 1). This result suggests that device aging at room temperature is not caused by morphological changes in the HTL or degradation at the indium-tin-oxide (ITO)–HTL interface. This is not necessarily the case for hole transport molecules with low glass transition tempera-

---

[1] Department of Materials Science and Engineering, McMaster University, Hamilton, Ontario, Canada. [2] Xerox Research Centre of Canada, Mississauga, Ontario, Canada.

*To whom correspondence should be addressed.

tures, particularly if devices are operated or stored at higher temperatures. The fact that the stability of the OLEDs can be enhanced by altering the HTL-AlQ$_3$ interface, by inserting a mixed layer in between, indicates that aging in OLEDs is mainly caused by degradation at (or near) that interface.

We investigated the enhanced stability of the OLEDs having a mixed layer by studying OLEDs with various structures. These included devices with a CuPc buffer layer at the ITO contact (*9*) and rubrene-doped HTL (*8*). The current density versus voltage (*J-V*) and luminance versus current density (*L-J*) characteristics of these devices are shown in Fig. 2. The characteristics of standard bilayer OLEDs, made from the same materials and fabricated on the same substrates during the same vacuum cycle, are also shown as a reference. The introduction of a 15-nm-layer of CuPc at the ITO contact enhances the EL efficiency (about 4.2 cd/A for OLEDs with the CuPc layer compared with about 3.1 cd/A for regular bilayer OLEDs). Because introducing the CuPc layer causes a shift in the *J-V* characteristics to higher voltages, it can be concluded that the CuPc impedes hole injection into the HTL. The higher EL efficiency is therefore attributed to the role of the CuPc in achieving more balanced electron and hole injection processes by impeding hole injection into the *N,N'*–di(naphthalene-1-yl)-*N,N'*-diphenylbenzidine (NPB) (*14*). Doping the HTL with rubrene also leads to a shift in the *J-V* characteristics of the OLEDs to higher voltages, in agreement with the findings of Vestweber and Rieb (*14*). This shift points to the role of the dopant molecules in forming hole traps, thus reducing their mobility in the HTL (*15*). Similar to the case of OLEDs with a CuPc layer, doping the HTL also leads to a higher EL efficiency. However, unlike CuPc, where the higher efficiency can be attributed solely to a more balanced electron/hole ratio, the role of dopant molecules in enhancing the efficiency must be extended to include their role in generation of light (*8*). The more pronounced shift in the *J-V* characteristics after introducing the CuPc layer than for doping the HTL can be attributed to the different nature of the hole-impeding process in both cases. The CuPc layer impedes the injection of holes into the HTL, but the dopant molecules reduce their mobility inside the HTL, the effect of which may not be as strongly reflected on the *J-V* characteristics because of the superior hole mobility characteristics of NPB (*16*). The shift of the *J-V* characteristics to higher voltages in the case of introducing the CuPc layer or doping the HTL does not contradict the lower luminance turn-on voltage achieved with these stabilizing agents due to efficiency enhancement. A common feature of the role of these two stabilizing agents is to impede the holes and thus to slow down their transport to the HTL-AlQ$_3$ interface where they are injected into the AlQ$_3$ layer. Thus hole injection into the AlQ$_3$ layer appears to be the main factor responsible for OLED degradation. This explanation is consistent with the results of Papadimitrakopoulos *et al.* (*17*), which show from cyclic voltammetry on AlQ$_3$ in solutions that oxidation of AlQ$_3$ is irreversible.

We then constructed devices in which predominantly holes are transported through a thin AlQ$_3$ layer (Fig. 3). A 5-nm-thick AlQ$_3$ layer was placed between two layers of NPB. The lower 20-nm-thick NPB layer facilitates the injection of holes from the ITO anode into the AlQ$_3$ layer, whereas the upper 40-nm-thick layer both transports the holes from the AlQ$_3$ layer to the cathode and blocks electrons from reaching the AlQ$_3$ layer. The blocking of electron transport by NPB was incomplete, however. Some electrons still reached the middle AlQ$_3$ layer and caused weak EL. Because the NPB-cathode contact was unstable, usually creating shorted devices, a thin buffer layer of AlQ$_3$ (10 nm thick) was used between the upper NPB layer and the cathode.

In situ PL measurements (performed with 442-nm Hg-line excitation, where NPB absorption is negligible) were carried out to monitor changes in the PL quantum efficiency of the 5-nm-thick AlQ$_3$ layer. A gradual decrease in the peak height of the PL spectra of AlQ$_3$ [Fig. 4, spectra (a) to (c)] revealed a continuous decrease in the PL efficiency of AlQ$_3$ after prolonged current flow. Other OLEDs consisting of only a 60-nm-thick NPB layer and a 10-nm-thick AlQ$_3$ top layer were also tested under the same conditions to determine whether PL from the top AlQ$_3$ contributed to the signal [Fig. 4, spectrum (d)]. The 10-nm AlQ$_3$ top layer, in contact with the metal cathode, contributes negligibly, probably because of exciton quenching by the metal due to the relatively large exciton diffusion length of AlQ$_3$ (*1*). Thus spectra (a) to (c) in Fig. 4 correspond to PL of the 5-nm AlQ$_3$ layer. The decrease in the PL

Fig. 1. Luminance (L)/initial luminance (L_o) and driving voltage (V)/initial driving voltage (V_o) versus time of a mixed emitting layer OLED (squares) and a standard bilayer OLED (triangles), both driven at 25 mA/cm^2. L_o values are 1050 and 710 cd/m^2 and V_o values are 7.5 and 8.0 V, respectively.

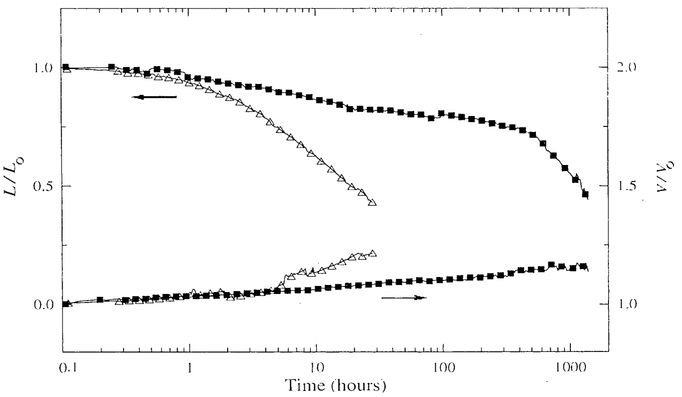

Fig. 2. *J-V* (**A**) and *L-J* (**B**) characteristics for ITO–NPB–AlQ$_3$–Mg-Ag (open circles), ITO-rubrene–doped NPB–AlQ$_3$–Mg-Ag (solid circles), and ITO–CuPc (15 nm)–NPB–AlQ$_3$–Mg-Ag (triangles) OLEDs. In all devices, the thicknesses of the HTL and AlQ$_3$ layers are 60 and 75 nm, respectively.

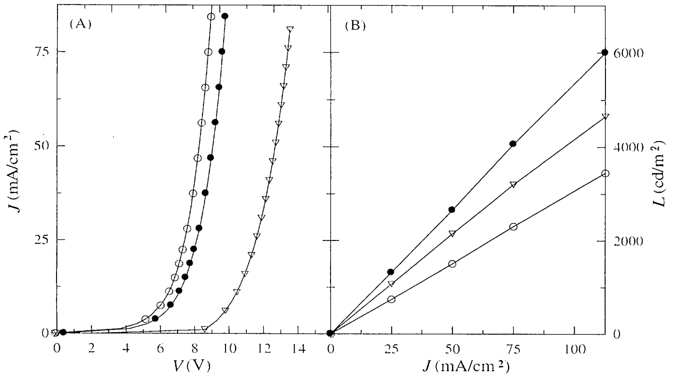

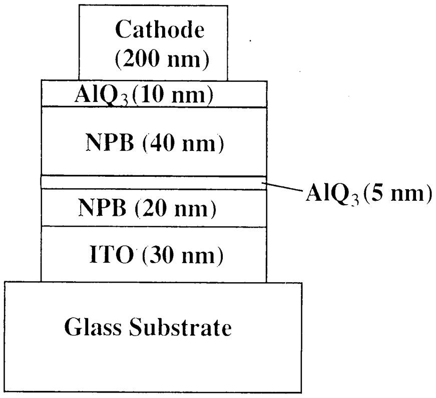

Fig. 3. Structure of OLEDs used for PL measurements.

quantum efficiency of this layer points to degradation as a result of current flow. As this layer transports predominantly holes, the observed fluorescence decrease indicates that cationic AlQ$_3$ species are most likely leading to formation of fluorescence quenchers. In principle another mechanism of fluorescence decrease is also possible—formation of a high concentration of nonemitting degradation products, which are not fluorescence quenchers. This mechanism would require that in our experiments (Fig. 4) about half the AlQ$_3$ molecules decompose. We investigated this possibility by using infrared spectroscopy to detect any changes in the absorption spectra of AlQ$_3$ after degradation. No detectable changes were observed, thus showing that the number of degraded AlQ$_3$ molecules is not substantial but is limited to a few that acted as fluorescence quenchers.

Identical devices in which the Mg-Ag cathodes were replaced by pure Ag cathodes were fabricated and tested under the same current driving conditions. Because of the higher work function of Ag compared with Mg-Ag (4.2 and 3.7 eV, respectively), the injection of electrons from the cathode into the organic layers is reduced, which leads to even more unbalanced current with higher hole/electron ratios. In the case of the devices with the Ag cathode, the PL intensity of the AlQ$_3$ decreased to 45% of the initial level [Fig. 4, spectrum (e)]. In comparison, when a Mg-Ag cathode was used, PL decreased less, to 60% of the initial value over the same time [Fig. 4, spectrum (c)]. This result clearly shows that higher hole/electron ratios lead to faster degradation of the AlQ$_3$, thus supporting the conclusion that cationic AlQ$_3$ species are unstable.

Because AlQ$_3$ is an excellent ETL (*18*), electron transport is not expected to cause degradation. Our studies on similar devices in which AlQ$_3$ layers were placed between two ETLs, thus allowing only electrons to be transported through the AlQ$_3$, did not show any decrease in the PL quantum efficiency under similar current driving conditions.

The role of doping the HTL or introducing a thin buffer layer of CuPc at the hole-injecting contact in improving OLED stability can be explained in terms of slowing down the hole transport to the HTL-AlQ$_3$ interface. Under these conditions, the density of electrons in the AlQ$_3$ layer adjacent to the HTL-AlQ$_3$ interface is increased, thus leading to rapid recombination and therefore a shorter lifetime of the unstable cationic AlQ$_3$ species. It is also possible that because of the high electron density at the HTL-AlQ$_3$ interface, the production of cationic AlQ$_3$ species is greatly reduced, as holes can be injected directly from NPB into anionic AlQ$_3$ species to produce excited states (*19*). This last effect is probably the dominant mechanism for improved stability of OLEDs with a mixed layer. In addition to improved carrier balance, holes in the mixed layer will preferentially reside on NPB sites because of the lower ionization potential of the NPB relative to that of AlQ$_3$ (5.1 and 5.6 eV, respectively), whereas electrons will reside on AlQ$_3$ sites. As NPB and AlQ$_3$ molecules are in close contact in the mixed layer, the direct recombination of holes and AlQ$_3$ anions to produce excited states of AlQ$_3$ directly will be a dominant recombination process.

The above argument can also be used to explain other phenomena pertaining to OLED stability. For example, the correlation between a lower ionization potential of the hole transport material and a higher device stability (*11*) can be explained in terms of the same processes. In this case, a lower ionization potential of the HTL leads to a more difficult injection of holes into the AlQ$_3$ as a result of a higher hole injection barrier at the HTL-AlQ$_3$ interface. The reduced injection of holes into the AlQ$_3$ layer leads to a higher density of electrons in the AlQ$_3$ layer adjacent to the HTL-AlQ$_3$ interface, which, in turn, leads to a shorter lifetime of cationic AlQ$_3$ species. The increase in device stability on using metals with lower work function for the cathodes (*20*) can be explained in terms of an easier injection of electrons from the cathode into the AlQ$_3$ layer, which leads to a higher density of electrons in the AlQ$_3$ layer adjacent to the HTL-AlQ$_3$ interface and hence a higher device stability.

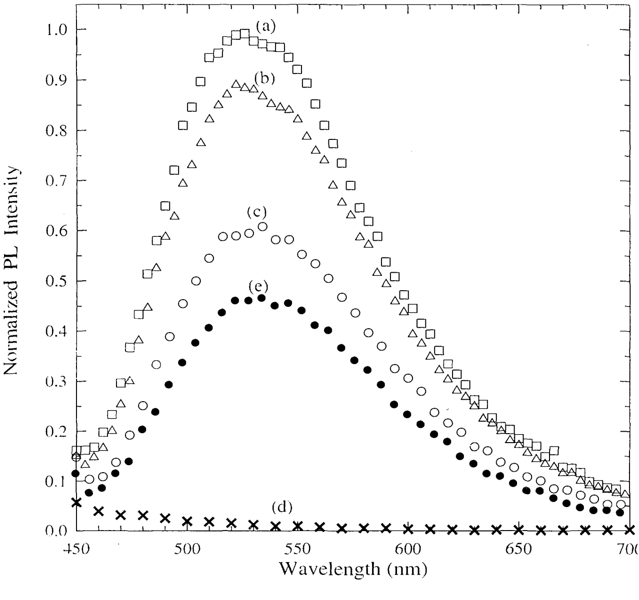

Fig. 4. Normalized PL spectra of AlQ$_3$ in a device from Fig. 3 with a Mg-Ag cathode, driven at 50 mA/cm^2, obtained before stressing (a), after stressing for 10 hours (b), and after stressing for 50 hours (c). Spectrum (d) was obtained from an OLED without the middle AlQ$_3$ layer. Spectrum (e) is a PL spectrum of a device from Fig. 3 with an Ag cathode, obtained after stressing for 50 hours. Spectra (b) to (e) are normalized to the peak PL before stressing the devices.

References and Notes

1. C. W. Tang, S. A. Van Slyke, C. H. Chen, *Appl. Phys. Lett.* **65**, 3610 (1989).
2. J. Kido and Y. Iizumi, *ibid.* **73**, 2721 (1998).
3. Z. Shen, P. E. Burrows, V. Bulović, S. R. Forrest, M. E. Thompson, *Science* **276**, 2009 (1997).
4. J. R. Sheats *et al.*, *ibid.* **273**, 884 (1996).
5. J. McElvain *et al.*, *J. Appl. Phys.* **80**, 6002 (1996).
6. H. Aziz *et al.*, *Appl. Phys. Lett.* **72**, 756 (1998); *ibid.*, p. 2642.
7. P. E. Burrows *et al.*, *ibid.* **65**, 2922 (1994).
8. Y. Hamada, T. Sano, K. Shibata, K. Kuroki, *Jpn. J. Appl. Phys.* **34**, L824 (1995).
9. S. A. Van Slyke, C. H. Chen, C. W. Tang, *Appl. Phys. Lett.* **69**, 2160 (1996).
10. J. Shi and C. W. Tang, *ibid.* **70**, 1665 (1997).
11. C. Adachi, K. Nagai, N. Tamoto, *ibid.* **66**, 2679 (1995).
12. OLEDs were made by using AlQ$_3$ as an emitting ETL, NPB as a HTL, ITO as an anode, and Mg-Ag as a cathode. All layers were deposited by vacuum evaporation at 6×10^{-6} torr on ultraviolet ozone cleaned ITO-patterned glass substrates. Organic layers were deposited at a rate of 0.2 to 0.4 nm/s. In the case of OLEDs with doped HTL, NPB containing about 1 mole percent of rubrene (5,6,11,12-tetraphenylnaphthacene) layers were formed by coevaporation from separate sources. After deposition of the organic layers, 200-nm-thick cathodes were made by coevaporation of Mg and Ag (deposited at 0.9 and 0.1 nm/s, respectively) without breaking the vacuum. *J-V* and *L-J* characteristics were measured with a Keithley 238 source-measure unit and a calibrated photodiode. Lifetime tests were carried out under constant (dc) current conditions, and PL spectra were obtained by using a Products for Research 191933-93 cooled photomultiplier, Oriel Hg arc lamp excitation source, and two Instruments SA monochromators (DH-10 for illumination and DH-20 for light detection). A Nicolet Magna-IR 550 spectrometer and IR PLAN microscope system were used for infrared measurements. All tests were carried out with devices continuously purged with dry N$_2$.
13. Z. D. Popovic *et al.*, in *Proc. SPIE, Organic Light-Emitting Materials and Devices II*, San Diego, CA, July 1998, vol. 3476, pp. 68–73.
14. H. Vestweber and W. Rieb, *Synth. Met.* **91**, 181 (1997).
15. J. Yang and J. Shen, *J. Appl. Phys.* **84**, 2105 (1998).
16. G. G. Malliaras and J. C. Scott, *ibid.* **83**, 5399 (1998).
17. F. Papadimitrakopoulos, X.-M. Zhang, D. L. Thomsen III, K. A. Higginson, *Chem. Mater.* **8**, 1363 (1996).
18. L. B. Bin, S. A. Jenekhe, R. H. Young, P. M. Borsenberger, *Appl. Phys. Lett.* **70**, 2052 (1997).
19. J. D. Anderson *et al.*, *J. Am. Chem. Soc.* **120**, 9646 (1998).
20. M. Matsumura and Y. Jinde, *Synth. Met.* **91**, 197 (1997).
21. Supported in part by the Natural Science and Engineering Research Council of Canada and the Ontario Graduate Scholarship program.

11 December 1998; accepted 10 February 1999